

Precision measurements of inclusive hadron production in pp and pC interactions at the CERN SPS

Martin MAKARIEV*

Bulgarian Academy of Sciences

E-mail: martin.makariev@cern.ch

In the framework of a general study of hadron production in elementary and nuclear interactions at the CERN SPS the NA49 experiment has produced new and complete sets of inclusive meson and baryon cross sections in p+p and p+C interactions. This work is aimed at providing precision data over most of the available phase space with a special emphasis on completeness, internal consistency and on the comparison to a wide range of existing experimental results. The corresponding physics analysis allows for a model-independent study of soft hadronic production with a view to a critical assessment of the applicability of the current approaches to the non-perturbative sector of QCD. In this context the precision study of p+A interactions opens a new access to the scrutiny and understanding of multiple hadronic collisions concerning specifically detailed nuclear and isospin effects including strangeness. In addition these data may serve as a reference for neutrino and astro-particle physics.

The European Physical Society Conference on High Energy Physics

18-24 July, 2013

Stockholm, Sweden

*Speaker.

1. Introduction

In the absence of quantitative predictions in the non-perturbative sector of QCD, the study of soft hadronic physics has to rely on self-consistent high statistics data sets, including a variety of projectile and target combinations. In addition full phase space coverage with complete particle identification and small systematic uncertainty are required.

The NA49 experiment aims at providing such data sets ranging from elementary hadron-proton collisions to hadron-nucleus and nucleus-nucleus interactions, obtained using the same detector layout combining wide acceptance, systematic uncertainty of less than 3% and complete particle identification via measurement of specific energy loss. It is therefore well suited for the comparison of the different processes and to a detailed scrutiny of the evolution from elementary to nuclear hadronic phenomena and thus providing a basis for a model independent study of the underlying production mechanisms.

In the framework of this extensive experimental program the NA49 experiment has already published papers concerning pion [1], baryon [2] and kaon [3] production in p+p collisions, and pion and baryon production [4, 5, 6, 7] in p+C collisions. In this paper the study of baryon production and new results of kaon production in p+C collisions will be discussed.

2. Data sets

The data sets obtained by the NA49 experiment at the CERN SPS at 158 GeV/c beam momentum are summarized in Fig. 1.

hadron-proton	hadron-nucleus	nucleus-nucleus
p + p	d + p	Pb + Pb
n + p	p + C	
π^+ + p	p + Pb	
π^- + p	π^+ + Pb	
	π^- + Pb	

Table 1: The data sets obtained by the NA49 experiment at 158 GeV/c beam momentum

3. Variables and cross section definition

The NA49 experiment establishes the invariant double differential cross sections

$$f(x_F, p_T) = E(x_F, p_T) \cdot \frac{d^3\sigma}{dp^3}(x_F, p_T). \quad (3.1)$$

Here p_T is the transverse momentum and x_F is the reduced longitudinal momentum:

$$x_F = \frac{p_L}{\sqrt{s}/2} \quad (3.2)$$

where p_L denotes the longitudinal momentum component in the center-of-mass system (cms). For the neutrons, due to the lack of transversal granularity of the NA49 calorimeter, only p_T -integrated density distributions:

$$dn/dx_F = \pi/\sigma_{\text{inel}} \cdot \sqrt{s}/2 \cdot \int f/E \cdot dp_T^2 \quad (3.3)$$

will be presented, with σ_{inel} being the total inelastic cross section.

4. Baryon production

4.1 Double differential and p_T integrated distributions

Double differential inclusive cross sections of protons and anti-protons have been derived in both p+p [2] and p+C [6] interactions. The results feature wide phase space coverage, from -0.8 to 0.95 in x_F and from 0 to 1.9 GeV/c in p_T for protons and from -0.2 to 0.4 in x_F and from 0 to 1.5 GeV/c in p_T for anti-protons, and systematic errors of 4% or less. An example of proton x_F distributions in p+C collisions is shown in Fig. 1. Existing data [8], which are complementary to the NA49 measurements in the far backward hemisphere were used to extend the coverage into the region of intra-nuclear cascading, see [6]. The corresponding x_F distributions cover the phase

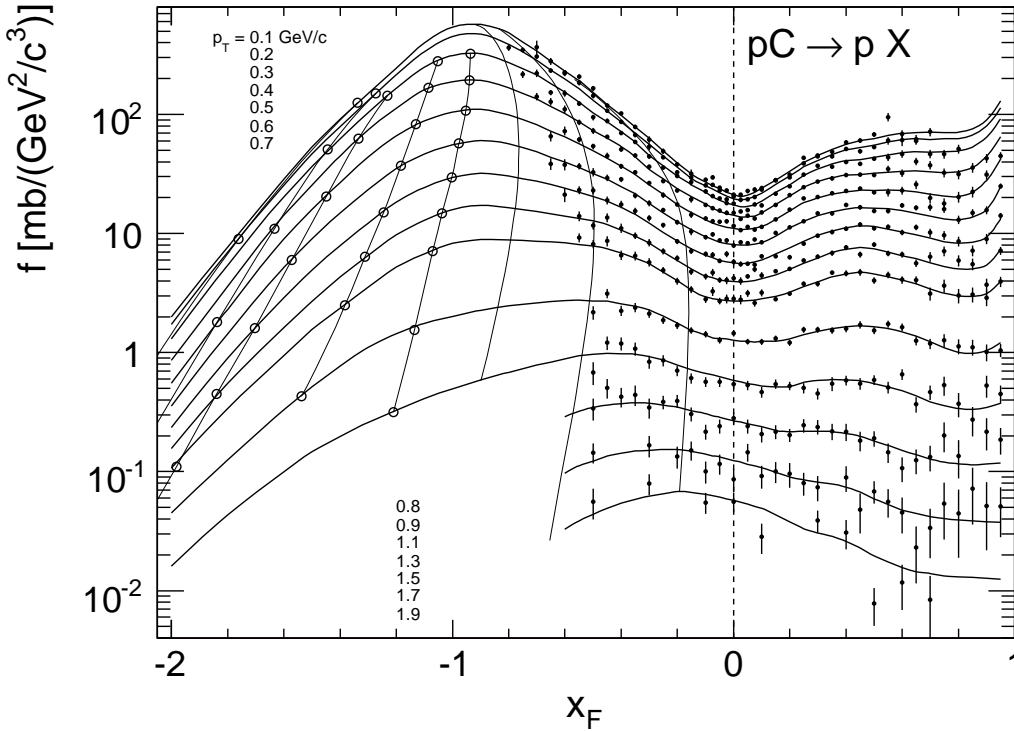


Figure 1: Invariant cross sections at fixed p_T as a function of x_F for protons in p+C collisions at 158 GeV/c beam momentum. Full circles: NA49 data, open circles: data from [8]. The thin lines show the cross section at fixed angles of 10° , 30° and 50°

space from $x_F = -2$ up to the kinematic limit at $x_F \sim +1$. Both the NA49 data (full circles) and [8] (open circles) are plotted.

The p_T integrated density distribution dn/dx_F for neutrons are also available from NA49 experiment for both p+p and p+C interactions [2, 6]. They are presented in Fig. 2 together with the p_T integrated densities for protons and anti-protons.

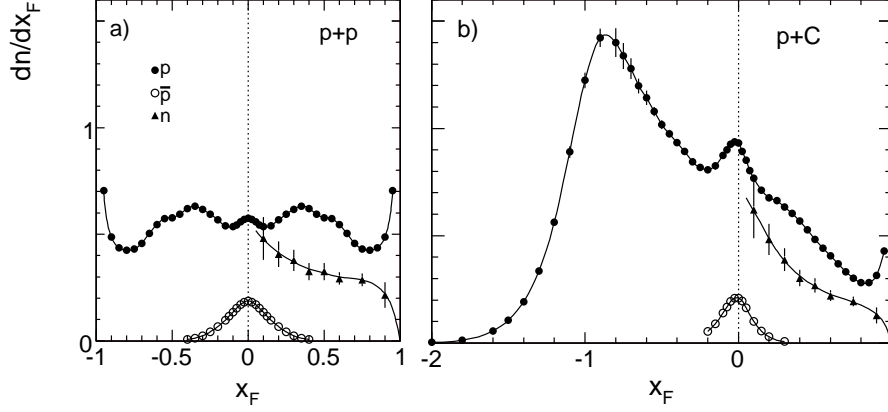


Figure 2: The p_T integrated density distribution dn/dx_F for protons, anti-protons and neutrons as a function of x_F in a) p+p collisions and b) p+C collisions. In panel a) the results for protons and anti-protons at positive x_F are reflected into negative x_F

4.2 Three component mechanism

The final state of p+A collisions consists of three basic components:

- The fragmentation of the projectile particle
- The fragmentation of the target nucleons
- The intra-nuclear cascading, generated by the interaction of the participating nucleons and secondary produced hadrons inside the nucleus.

The separation and extraction of these three components can be done relying only on the experimental data. To achieve this one can define "net" baryon production which is the difference between the total yield and the pair produced baryons of the same type. In the case of protons, the pair produced protons can be extracted from measured anti-proton yields taking into account the isospin symmetry. Then the overlap function between target and projectile fragmentation of "net" protons, which obeys baryon number conservation, can be extracted by fixing a baryon at large $|x_F|$ and studying the correlation function ρ^c . The ratio of correlated and inclusive cross sections ρ^c/ρ^{incl} for forward and backward selection of baryons in p+p collisions is shown in Fig. 3. In the two cases this ratio equals to 0.5 at $x_F = 0$ and reaches values of 0 or 1 at x_F of about 0.2.

A similar extraction can be performed also in p+C collisions, see [6]. As in p+C collisions there is a third component, namely the nuclear cascading, an assumption about the target component has to be made. The target component can be predicted from p+p interaction by forming

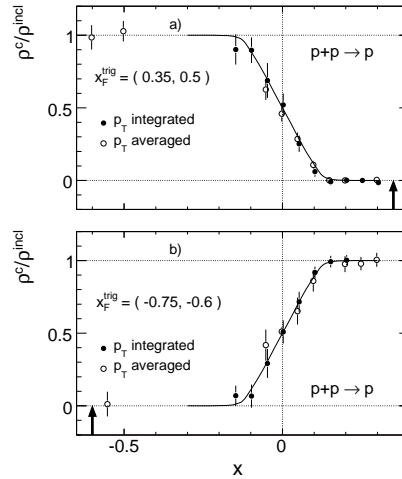


Figure 3: p_T integrated and p_T averaged constrained net proton density ratios $R_p^{c.net}$ as a function of x_F , a) for forward net proton selection and b) for backward net proton selection. The full lines shown represent the overlap functions and arrows indicate the x_F of the tagging baryon

the isospin average between net neutron and net proton densities and multiplying this average by the mean number of collisions $\langle v \rangle$ in p+C interactions. $\langle v \rangle$ is measured to be 1.6, [5]. With this assumption for the target fragmentation one can extract the three independent components in p+C collisions as shown in Fig. 4b. In Fig. 4a the result in p+p collisions is presented.

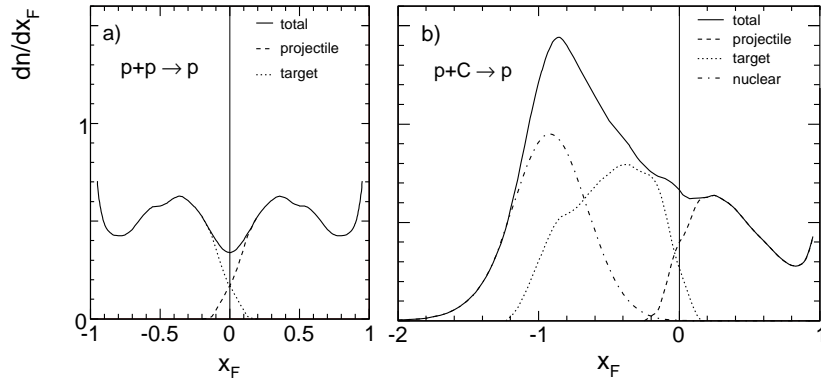


Figure 4: The independent components for net protons in a) p+p and b) p+C collisions

5. Meson production

5.1 Double differential distributions

Inclusive meson cross section have already been published by the NA49 experiment – pions in p+p [1] and p+C [1] collisions and kaons in p+p [3]. New results on kaon production as a function of x_F in p+C collisions are presented in Fig. 5. The data cover a wide kinematic range from -0.4 to 0.4 in x_F and from 0 to 1.5 GeV/c in p_T .

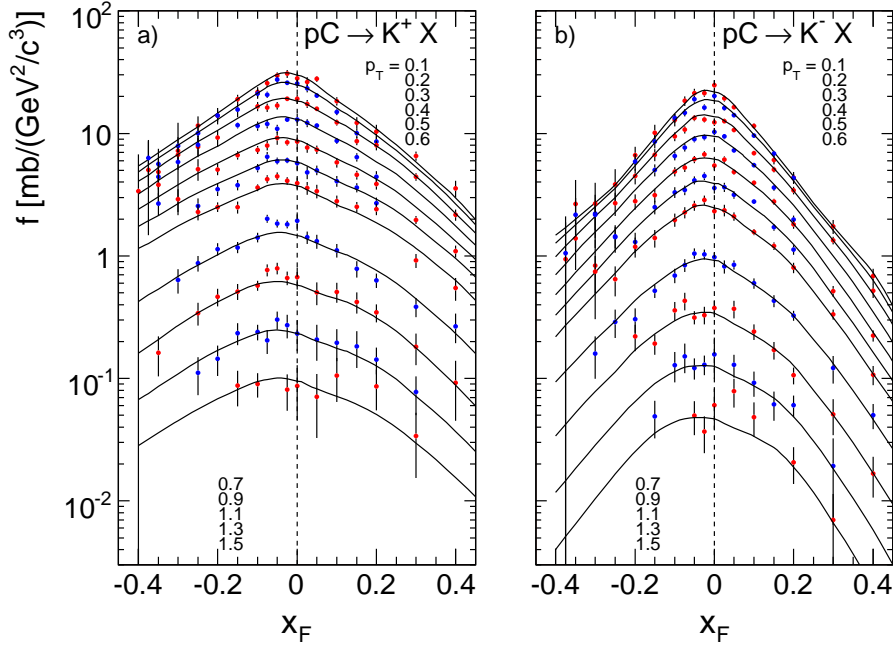


Figure 5: Invariant cross sections at fixed p_T as a function of x_F for a) K^+ and b) K^- in p+C collisions at 158 GeV/c beam momentum

5.2 Particle ratio

Using the above results one can form π^+/π^- and K^+/K^- ratios. They are shown in Fig. 7, where results from [7] and measurements from Fermilab in p+p [9] and p+Ta [10] interactions are used to extend the x_F range.

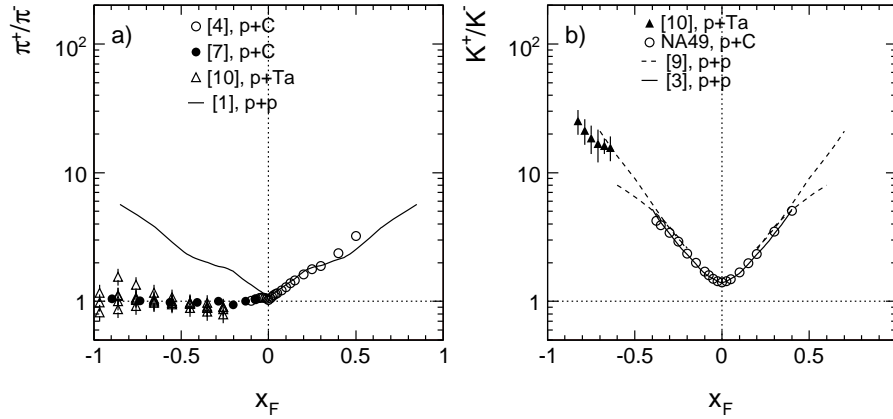


Figure 6: Mesonic charge ratios in the nuclear fragmentation region of p+C and p+Ta interactions as a function of x_F . Panel a) π^+/π^- , panel b) K^+/K^- . The results from p+p collisions are shown as full lines for π^+/π^- [1] and K^+/K^- [3] and several Fermilab experiments [9, 10] (broken lines)

A distinctive difference in the behaviour of pion and kaon ratios in the target hemisphere in p+A collisions is observed. While the π^+/π^- ratio is close to 1, the K^+/K^- ratio reaches values of

more than 20 and reproduces the ratio found in p+p interactions. This striking difference is due to the different production mechanism of pions and kaons.

This observation has an important consequence for the interpretation of K^+/π^+ ratios when passing from p+p to p+A interactions. An example of K^+/π^+ ratios as a function of x_F at $p_T = 0.3$ GeV/c in p+p and p+C collisions is shown in Fig. 7. Here the increase of the ratio at negative x_F in p+C collisions can be wrongly interpreted as "strangeness enhancement", while it is entirely due to the isospin effect.

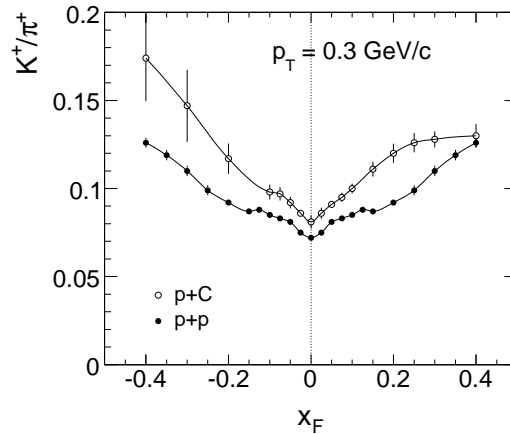


Figure 7: Ratio K^+/π^+ as function of x_F at $p_T = 0.3$ GeV/c in p+p and p+C collisions

6. Conclusions

New results from NA49 experiment on inclusive production of mesons and baryon in p+p and p+C collisions at 158 GeV/c beam momentum are presented. The three independent components of hadronization in p+C collisions are extracted experimentally. The importance of isospin effects for the interpretation of the K^+/π^+ ratio when passing from p+p to p+A interactions is demonstrated.

References

- [1] C. Alt et al., Eur. Phys. J. **C45** (2006) 343
- [2] T. Anticic et al., Eur. Phys. J. **C65** (2010) 9
- [3] T. Anticic et al., Eur. Phys. J. **C68** (2010) 1
- [4] C. Alt et al., Eur. Phys. J. **C49** (2007) 897
- [5] G. Barr et al., Eur. Phys. J. **C49** (2007) 919
- [6] B. Baatar et al., Eur. Phys. J. **C73** (2013) 2364
- [7] O. Chvala et al., Eur. Phys. J. **C73** (2013) 2329
- [8] Y. D. Bayukov et al., Phys. Rev. **C20**, (1979) 764
- [9] A. E. Brenner et al., Phys. Rev. **D26** (1982) 1497
J. R. Johnson et al., Phys. Rev. **D17** (1978) 1292
- [10] N. A. Nikiforov et al., Phys. Rev. **C22** (1980) 700